VI. Conclusion

We note in the theoretical calculations that $\Delta\theta = 3.5°$ was obtained which is reasonably close to the experimental measurements of $\Delta\theta \approx 5.0°$. We conclude that (1) and (2) are valid approximations. A further conclusion is that for large insulator spacing between the runner and p-i-n diode modulator and with the diode unbiased, only a small edge of the evanescent wave interacts with the p-i-n modulator. Since the coupling is small, the wave is relatively undisturbed. With full forward bias applied to the p-i-n diode, a conductive wall forms and changes the transmitted wavelength. Due to the relatively thick insulator layer, the interaction is so small that refraction does not significantly occur although a slight amount of absorption still results. In this condition, a small amount of angular scan can occur and with low attenuation and negligible beam spreading. This is verified by analysis of the experimental data which shows that as the forward bias current is increased in small increments, the radiated beam starts to shift with some attenuation. As the current is increased to 50 mA and above, the angular shift increases to its maximum value and the attenuation is reduced to almost zero as it was with zero bias current. It should be noted that the analog effect starts to occur for low current levels of 1 mA. Above 50 mA, no further effect is observed. This indicates that diodes become conductive at very low-current levels and reach a maximum conducting level at less than 25 mA per diode.

Acknowledgment

The authors wish to acknowledge help from Dr. F. Schwering for consultation on the analysis and to E. Malecki for construction of the p-i-n diodes.

References

[1] R E Horn, H. Jacobs, E Freibergs, and K. L. Klohn, "Electronic modulated beam-steerable silicon waveguide array antenna," *IEEE Trans. Microwave Theory Tech.*, vol. MTT-28, pp 647–653, June 1980.
[2] H. Jacobs and F. K. Schwering, private communication
[3] A. A. Oliner, Polytechnic Institute of New York, private communication.
[4] E. A. J. Marcatili, "Dielectric rectangular waveguide and directional coupler for integrated optics," *Bell Syst. Tech. J.*, vol. 48, no 7, Sept 1969.

Diffraction Loss in Dielectric-Filled Fabry–Perot Interferometers

PAUL F. GOLDSMITH, MEMBER, IEEE

Abstract—**We analyze the transmission of dielectric-filled Fabry–Perot interferometers excited by a spherical wave having a Gaussian amplitude distribution transverse to the axis of propagation. The loss due to diffraction experienced by the incident mode is found to be reduced by a factor $\geq n^4$ when n, the index of refraction of the dielectric, is significantly greater than unity, thus permitting such devices to be used with low loss in beams of considerably greater angular divergence than possible with air-filled interferometers. Measurements at 3-mm wavelength of devices made of quartz and sapphire are presented, which are in good agreement with the theoretical calculations.**

Manuscript received October 19, 1981; revised December 1, 1981 This work was supported in part by the National Science Foundation under Grant AST 80-26702 This is contribution Number 499 of the Five College Observatory.

The author is with the Five College Radio Astronomy Observatory, 619 Graduate Research Center, University of Massachusetts, Amherst, MA 01003.

I. Introduction

Fabry–Perot interferometers have been employed at millimeter wavelengths as single-sideband filters [1], [2], and as local oscillator injectors [2], [3]; the primary incentive for their use is the lower loss obtainable with quasi-optical devices compared to their waveguide analogs used at lower frequencies. In order to achieve a high level of performance, the effects of diffraction must be considered; these impose a lower limit to the beam diameter that can be employed. The effects of diffraction on Fabry–Perot interferometer performance at microwave frequencies have been treated in considerable detail by Arnaud, Saleh, and Ruscio [4] (hereafter ASR). These authors treat the diffraction loss at normal incidence, as well as the additional walk-off loss that occurs at oblique incidence. In the present work, we extend their formulation to explicitly include dielectric-filled interferometers, and present some design curves for calculating the transmission of the fundamental mode under excitation by a gaussian beam.

II. Fabry–Perot Interferometer

A. Geometrical Optics Limit

The Fabry–Perot interferometer is considered to consist of two infinite plane mirrors, each having power reflectivity $R = |\rho e^{i\phi_r}|^2$, where ρ is the amplitude, and ϕ_r the phase of the electric field reflection coefficient. The mirrors are considered to be lossless, that is, $R = 1 - T$, where T is the power transmission coefficient. We define $T = |te^{i\phi_t}|^2$, t, and ϕ_t being the magnitude and phase of the field transmission. In the absence of diffraction (plane wave or geometrical optics limit) the fraction of incident power transmission is given by [5]

$$|\tau|^2 = \frac{\xi^2\left(\frac{1-R}{1-\xi^2 R}\right)^2}{1+\frac{4\xi^2 R}{(1-\xi^2 R)^2}\sin^2(\delta\phi/2)} \tag{1}$$

where ξ^2 is the one-way power transmission of the medium between the mirrors, and $\delta\phi$ is the round-trip phase delay. The round-trip phase delay is

$$\delta\phi = 2\phi_r + (4\pi d/\lambda)(n^2 - \sin^2 i)^{1/2} \tag{2}$$

for an interferometer with mirror spacing d, a medium between the mirrors having index of refraction n, and with the direction of the incident radiation being at an angle i from normal incidence. For an interferometer consisting only of a slab of dielectric, the power reflection coefficient at each interface is obtained from the Fresnel equations [6], and $2\phi_r = 2\pi$. For mirrors consisting of metallic mesh, for example, the reflection coefficient and phase are more complicated and generally quite frequency-dependent [7].

B. Gaussian Beam Excitation

Many types of microwave feedhorns as well as beam-waveguide systems produce radiation patterns which can be reasona-

0018-9480/82/0500-0820$00.75 ©1982 IEEE

bly accurately described by a single Gaussian mode which has electric field amplitude transverse to the direction of propagation given by

$$E(r)/E(0)=\exp\left[-(r/w)^2\right] \tag{3}$$

r being the distance from the beam axis [8]. The beam radius w and the radius of curvature of the wavefront are functions of the distance from the beam waist, where w is equal to its minimum value w_0, called the waist radius [8], [9]. ASR [4] have shown that the response of the interferometer is independent of its location in a Gaussian beam, provided that the interferometer is much larger than the beam diameter at its location, and that w_0 is the only beam parameter affecting the interferometer response. The smaller w_0, the broader is the angular spectrum of plane waves present in the beam, and hence the ideal response given by (1) will be degraded.

III. Interferometer Response to Gaussian Beam

A. Initial Field Configuration

We consider a transmission system such as that shown in Fig. 1, designed so that the Gaussian beam produced by the feed $F1$ is perfectly coupled by means of focusing elements $L1$ and $L2$, to the feed $F2$; the relationships between the feed waist radii, lens focal lengths, and distances can be found in many references on Gaussian beam propagation [8], [9]. We first consider inserting a dielectric slab of thickness d, index of refraction n, at any position within the system, ignoring for the moment reflection at the interfaces. The beam propagation will be affected in two ways. In Fig. 2 we show schematically the dielectric slab inserted in the beam. A Gaussian beam propagating through a distance l of dielectric travels an effective distance $d_e=l/n$, in terms of the change in beam radius and wavefront radius of curvature [9]. The dielectric produces a change in the effective distance

$$\delta d_{eOD}=d\cos i\left(\frac{\cos i}{(n^2-\sin^2 i)^{1/2}}-1\right). \tag{4}$$

The separation between the waists must be increased to reestablish perfect coupling between the feeds. In addition, there is a lateral offset δy_{OD} shown in Fig. 2 which is given by

$$\delta y_{OD}=d\sin i\left(\frac{\cos i}{(n^2-\sin^2 i)^{1/2}}-1\right). \tag{5}$$

These changes will reduce the coupling between the feeds, if not compensated by the appropriate feed (and possibly lens) motion. The electric field coupling coefficient produced by a lateral offset δy and effective length error δd_e, for a Gaussian beam waist having a waist radius w_0 is [10]

$$c_{\delta y\,\delta d_e}=\frac{1}{1+\dfrac{i\lambda\,\delta d_e}{2\pi w_0^2}}\exp\left\{-\frac{\delta y^2}{2w_0^2}\left(\frac{1}{1+\dfrac{i\lambda\,\delta d_e}{2\pi w_0^2}}\right)\right\}. \tag{6}$$

The power coupling coefficient, which is the fraction of the incident power collected in the mode of the output beam is

$$K_{t0}=|c|^2. \tag{7}$$

If the relative location of the optical components is not adjusted, there is a mismatch between the beam having traversed the dielectric and the mode accepted by the remainder of the system, which should not be confused with possible loss due to the diffraction of the beam in the multiple passes through the interferometer. In most situations, since the number of passes is fairly large, the loss due to initial beam perturbations will be small compared to that resulting from the subsequent propagation, and can be neglected. In what follows, we will assume that the configuration is such that there is perfect transmission through the system with the (nonreflective) dielectric in place.

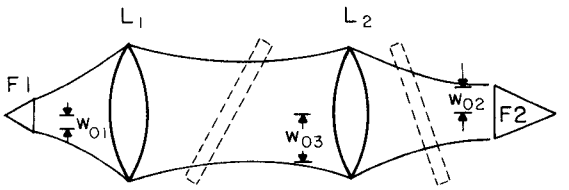

Fig 1 An example of transmission system sensitive to the transmission of fundamental Gaussian mode through Fabry–Perot interferometer. The focusing elements $L1$ and $L2$ can be lenses or mirrors with focal lengths and distances chosen to perfectly couple the Gaussian beam radiated by $F1$ [with waist radius (w_{01})] to $F2$ [which has waist radius w_{02}]. The Fabry–Perot interferometer is shown schematically in two possible positions; if located between L1 and L2 for example, the waist radius w_{03} would be used in (6) for calculating the loss to the fundamental mode.

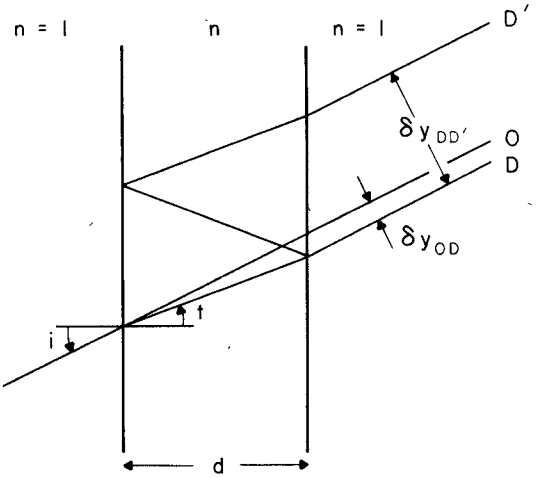

Fig 2. Effect of dielectric slab on paraxial ray representing the Gaussian beam. The initial insertion of the dielectric produces a lateral offset δy_{OD} and subsequent round trips produce an incremental lateral offset $\delta y_{DD'}$.

B. Effect of the Interferometer

Following ASR [4], we denote the initial electric field configuration as Ψ_0 and the configuration after s round trips through the interferometer as Ψ_s. The total electric field transmitted by the interferometer is

$$\Psi=\xi(te^{i\phi_t})^2\sum_{s=0}^{\infty}\left(\rho e^{i\phi_r}\right)^{2s}\xi^{2s}\Psi_s. \tag{8}$$

Note that Ψ_s includes the phase of the electric field after s round trips. The coupling coefficient between Ψ_s and Ψ_0 is given by (6), multiplied by the phase shift (2), where for each successive round trip the change in effective length is given by

$$\delta d_{eDD'}=\frac{2d(1-\sin^2 i)}{(n^2-\sin^2 i)^{1/2}} \tag{9}$$

and the incremental lateral offset (see Fig. 2) is

$$\delta y_{DD'}=\frac{2d\sin i\cos i}{(n^2-\sin^2 i)^{1/2}} \tag{10}$$

which is in the opposite sense of the initial offset δy_{OD}(5). The

total power transmission of the original Gaussian mode is then given by

$$K_{t0}=\left|\xi t^2 e^{2\iota\phi_t}\sum_{s=0}^{\infty}\rho^{2s}\xi^{2s}e^{\iota s\delta\phi}\frac{1}{1+\dfrac{is\lambda\delta d_{eDD'}}{2\pi w_0^2}}\right.$$

$$\left.\cdot\exp\left\{-\frac{s^2\delta y_{DD'}^2}{2w_0^2}\left(\frac{1}{1+\dfrac{is\lambda\delta d_{eDD'}}{2\pi w_0^2}}\right)\right\}\right|^2. \quad (11)$$

The value of the waist radius to be used is that for the section of the transmission system in which the interferometer is located.[1] If we define

$$D=\delta d_{eDD'}\left[T\left(\pi w_0^2/\lambda\right)\right]^{-1} \quad (12a)$$

and

$$G=\delta y_{DD'}\left[\sqrt{2}/w_0 T\right] \quad (12b)$$

(11) is seen to be a generalization of (22) of ASR [4]. The significance of the terms involving D and G, representing loss due to change in effective length and geometrical walkoff, respectively, is discussed in detail by ASR [4] and is no different for dielectric-filled Fabry–Perot interferometers than for their air-filled counterparts.

The effect of the dielectric can most clearly be seen in the reduction of the incremental lateral walkoff and the effective length per pass given by (9) and (10). The frequency interval between transmission maxima is determined by the requirement of a change in $\delta\phi$ of 2π. For a given interval $\delta\nu$ we can write

$$\delta y_{DD'}=\frac{(c/\delta\nu)\sin i\cos i}{n^2-\sin^2 i} \quad (13a)$$

$$\delta d_{eDD'}=\frac{(c/\delta\nu)(1-\sin^2 i)}{n^2-\sin^2 i} \quad (13b)$$

and hence we see that the reduction in these quantities is greater than or equal to a factor n^2 when compared to an air-filled interferometer. The use of dielectric-filled interferometers can thus make possible the use of devices which have unacceptable losses in their normal configuration.

The effect of diffraction can be conveniently assessed in terms of D, G, and T. Using (11) we have determined the maximum values of K_{t0}, assuming $\xi^2=1$. The maxima do not occur where $\delta\phi=0,2\pi,4\pi,\cdots$, as is the case in the absence of diffraction as given by (1) ([4], fig. 2). In Fig. 3(a) and (b) we have plotted the maximum transmission in the fundamental Gaussian mode as a function of D and G for several values of mirror power reflectivity R. These values fall below those for the total power transmission presented in a similar figure by ASR [4]. For small transmission losses and high mirror reflectivity, these authors have shown that

$$K_{t0}\simeq 1-(G^2+D^2). \quad (14)$$

[1]It should be noted that there can be partial cancellation of the coupling loss due to the initial insertion of the "reflectionless" dielectric and the loss due to the effect of the repeated bounces of the beam between the mirrors, as the signs of δy as well as δd_e are opposite for these two situations. In most practical situations the initial loss will be smaller; if this is not so, the loss calculated using (11) will exceed that which can be obtained by optimizing the coupling.

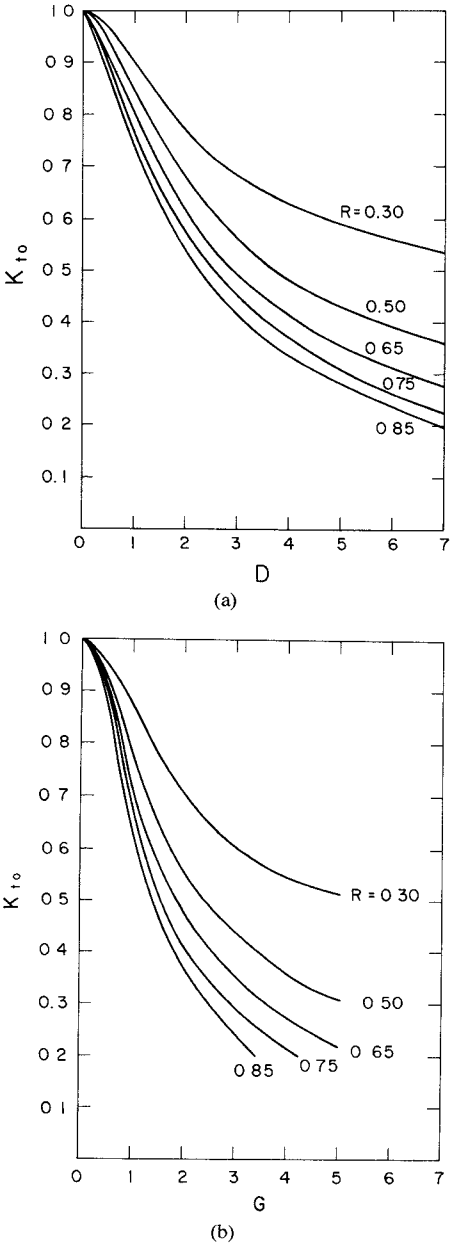

Fig. 3. Effect of Fabry–Perot interferometer on transmission of fundamental Gaussian mode K_{t0} shown as a function of mirror power reflectivity R. In (a) we consider the case of normal incidence so that $i=G=0$ [(9) and (12a)]. The parameter D is defined in (12a). In (b) we consider the effects of the geometrical walkoff alone, with the parameter G being defined in (12b). As discussed in the text, D and G are both decreased by a factor $\sim n^2$ for a dielectric-filled interferometer when compared to an air-filled device having the same spacing in frequency of transmission maxima.

In this case, we see that the loss due to the effects of diffraction will be reduced by a factor of approximately n^4 by using a dielectric-filled interferometer. This improvement will inevitably be offset by the dielectric absorption. The latter effect can be calculated using (11), but in general this will not be significantly different from that obtained from (1), from which

$$|\tau|^2(\mathrm{MAX})=\xi^2\left(\frac{1-R}{1-\xi^2 R}\right)^2 \quad (15a)$$

where

$$\xi^2=\exp\left[-2\pi n^2(d/\lambda)(n^2-\sin^2 i)^{-1/2}\tan\delta\right] \quad (15b)$$

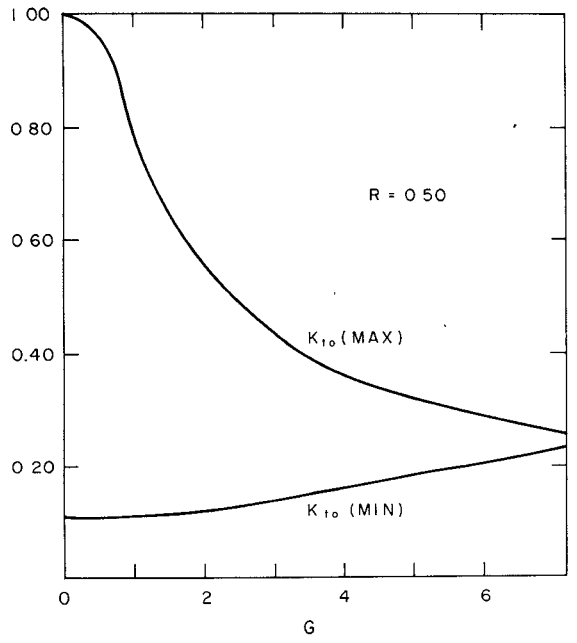

Fig. 4. Effect of walkoff loss on transmission maxima and minima of an interferometer with mirror power reflectivity = 0.5 The maximum transmission (denoted K_{t0}(MAX)) is seen to be much more rapidly degraded than is the minimum transmission K_{t0}(MIN).

$\tan\delta$ being the loss tangent of the dielectric, typically 10^{-4} to 10^{-3} for low-loss materials at millimeter and submillimeter wavelengths.

Diffraction of the radiation also has the effect of increasing the transmission minima of the interferometer. In Fig. 4 we give one example of the effect of walkoff on an interferometer with mirror reflectivity $R = 0.5$. In general, the effect on the minima can be neglected for K_{t0}(MAX) not too much less than 1, unless very high rejection is required.

C. Angle Tuning

Using the geometrical-optics limit for the response of a lossless interferometer, the fractional change in the resonant frequency is given by

$$\frac{1}{\nu}\frac{\partial \nu}{\partial i} = \frac{\sin i \cos i}{n^2 - \sin^2 i}(\text{rad}^{-1}). \tag{16}$$

This will generally be $\sim n^2$ smaller than for an air-filled device, making the dielectric-filled Fabry–Perot correspondingly less sensitive to changes in orientation. A wide tuning range can be obtained by utilizing a pair of wedged pieces of dielectric.

IV. Experimental Results

Two promising low-loss dielectric materials are fused silica ($n \sim 1.95$) and sapphire ($n \sim 3.2$), although little precise information is available on their properties between 50 and 500 GHz. We have carried out measurements on various samples of both of these materials using an experimental setup similar to that shown in Fig. 1. The signal source was a backward wave oscillator covering 80–100 GHz. The feeds were narrow flare-angle scalar feedhorns having $w_0 = 0.3$ cm, and the lenses, made of teflon, had a focal length of 8.5 cm. The waist radius between the lenses was 2.3 cm.

Several samples of quartz have been measured with results consistent with $n = 1.95$. The loss tangent was not accurately measured, but is < 0.0005 at 100 GHz.

The sample of sapphire measured, 0.50-cm thick, was measured at location A in Fig. 1. The crystal was cut so that the fast ($\epsilon = 11.66$) optical axis was inclined 60° to the perpendicular to the sample face; the slow ($\epsilon = 9.12$) axis is perpendicular to the fast axis. Thus, there are two polarizations separated by 90° having a well-defined propagation constant [11], for radiation traveling normal to the sample face. From the interferometer behavior, we deduce dielectric constants in good agreement with the submillimeter constants given above [12], with an accuracy of ± 0.2. The depths of the transmission minima are also consistent with these values.

At normal incidence $G = 0$ and $D = 0.008$ so that the expected value of K_{to} cannot be reliably distinguished from unity.[2] We can thus use the value of the transmission maxima to derive a value for the loss tangent with the result that $\tan\delta = 0.001 \pm 0.0005$. For $i = 45°$, $G = 0.164$, and for the perpendicular polarization, $K_{t0} = 0.98$. With the above value for $\tan\delta$ we compute the expected maximum transmission to be 0.91, in good agreement with the measured value of 0.90. The spacing of the maxima (9.1 GHz at 45° angle of incidence) would require an air-filled interferometer with a mirror spacing of 2.33 cm. The measured value of $R = 0.40$ would then give $G = 3.34$, and from Fig. 3(b) we find that the maximum value of K_{t0} would be only 0.5, thus illustrating the advantage of the dielectric-filled interferometer.

Acknowledgment

The author wishes to thank N. Erickson and R. Haas for valuable discussions, and to acknowledge the hospitality of the Institut de Radioastronomie Millimetrique, Grenoble, where part of this work was carried out. K. Breuer supplied the horns and lenses used in making the measurements.

References

[1] P. G. Wannier, J. A. Arnaud, F. A. Pelow, and A. A. M. Saleh, "Quasioptical band-rejection filter at 100 GHz," *Rev. Sci. Instr.*, vol. 47, pp. 56–58, 1976.

[2] P. F. Goldsmith, "A quasioptical feed system for radioastronomical observations at millimeter wavelengths", *Bell Syst. Tech. J.*, vol. 56, pp. 1483–1501, 1977.

[3] J. J. Gustincic, "Receiver design principles", in *Proc. Soc. Photo-Optical Instrum. Eng.*, vol. 105, pp. 40–43, 1977.

[4] J. A. Arnaud, A. A. M. Saleh, and J. T. Ruscio, "Walkoff effects in Fabry-Perot diplexers," *IEEE Trans. Microwave Theory Tech.*, vol. MTT-22, pp. 486–493, 1974.

[5] R. H. Garnham, "Quasi-optical components," in *Millimeter and Submillimeter Waves*. Ed., F. A. Benson, London: Iliffe, 1969, Ch 21.

[6] M. Born and E. Wolf, *Principles of Optics*. Oxford: Pergamon Press, 1975, Ch. 1.

[7] R. Ulrich, "Far infrared properties of metallic mesh and its complementary structure," *Infrared Phys.*, vol. 7, pp. 37–55, 1967.

[8] P. F. Goldsmith, "Quasioptical techniques at millimeter and submillimeter wavelengths," in *Infrared and Millimeter Waves* vol. 6, Ed K. J Button, New York: Academic, in press.

[9] H. Kogelnik and T. Li, "Laser beams and resonators," *Appl. Opt.*, vol. 5, no 10, pp. 1550–1567, 1966.

[10] H. Kogelnik, "Coupling and conversion coefficients for optical modes," in *Polytechnic Institute of Brooklyn Symposium on Quasi-Optics*. Brooklyn: Polytechnic Press, 1964, pp. 333–347.

[11] M Born and E. Wolf, *Principles of Optics*. Oxford: Pergamon Press, 1975, Ch. 14.

[12] E. V. Lowenstien, D. R. Smith, and R. L. Morgan, "Optical constants of far infrared materials; 2 crystalline solids," *Appl. Opt.*, vol. 12, pp. 398–406, 1973.

[2] The reduction of the coupling due to the initial insertion of the dielectric is also negligible in this case.